



Li, S., Xing, Y., Valdes, P. J., Huang, Y., Su, T., Farnsworth, A., Lunt, D. J., Tang, H., Kennedy, A. T., & Zhou, Z. (2018). Oligocene climate signals and forcings in Eurasia revealed by plant macrofossil and modelling results. *Gondwana Research*, 61, 115-127.  
<https://doi.org/10.1016/j.gr.2018.04.015>

Peer reviewed version

License (if available):  
CC BY-NC-ND

Link to published version (if available):  
[10.1016/j.gr.2018.04.015](https://doi.org/10.1016/j.gr.2018.04.015)

[Link to publication record in Explore Bristol Research](#)  
PDF-document

This is the author accepted manuscript (AAM). The final published version (version of record) is available online via Elsevier at <https://www.sciencedirect.com/science/article/pii/S1342937X18301473> . Please refer to any applicable terms of use of the publisher.

## University of Bristol - Explore Bristol Research

### General rights

This document is made available in accordance with publisher policies. Please cite only the published version using the reference above. Full terms of use are available:  
<http://www.bristol.ac.uk/red/research-policy/pure/user-guides/ebr-terms/>

**Oligocene climate signals and forcings in Eurasia revealed by plant  
macrofossil and modelling results**

Shufeng Li<sup>a,b</sup>, Yaowu Xing<sup>a,\*</sup>, Paul J. Valdes<sup>b</sup>, Yongjiang Huang<sup>c</sup>, Tao Su<sup>a</sup>, Alex Farnsworth<sup>b</sup>,  
Daniel J. Lunt<sup>b</sup>, He Tang<sup>a,d</sup>, Alan Kennedy<sup>b</sup>, Zhekun Zhou<sup>a,c,\*</sup>

<sup>a</sup>Key Laboratory of Tropical Forest Ecology, Xishuangbanna Tropical Botanical Garden,  
Chinese Academy of Sciences, Yunnan 666303, China

<sup>b</sup>School of Geographical Sciences, University of Bristol, Bristol, UK

<sup>c</sup>Key Laboratory of Biogeography and Biodiversity, Kunming Institute of Botany, Chinese  
Academy of Sciences, Kunming 650204, China

<sup>d</sup>University of Chinese Academy of Sciences, Beijing 100049, China

Correspondence: Yaowu Xing, tel. (fax): +86-691-8713882, e-mail: ywxing@xtbg.org.cn;  
Zhekun Zhou, tel. (fax): +86-691-8713226, e-mail: zhouzk@xtbg.ac.cn.

**Abstract**

The Oligocene represents a transitional time period from a warm climate to a cooler  
climate that is more representative of the modern day; yet, a general view of continental  
climate pattern and forcings are still lacking. Different proxies and models show striking  
disparities, especially in mid-high latitudes, requiring validation of Oligocene climate  
reconstruction in order to understand the large-scale processes that drive the observed climate  
changes. Here, we compiled 149 macrofossil floras in the mid-high latitudes of Eurasia, then  
quantitatively reconstructed the Oligocene climate using Coexistence Approach (CA) and  
combined previous published paleoclimate data. During the Oligocene, Eurasian mid-high

latitudes were mainly dominated by a humid subtropical climate. Mean annual temperature (MAT) ranged between 5.4 °C and 25.5 °C with mean annual precipitation (MAP) ranging from 338 to 2453 mm. Three regions (Europe, central Eurasia and eastern Asia) indicate different climatic regimes, with a generally warmer and wetter climate in Europe and a colder and drier climate in central Eurasia when compared to eastern Asia. No significant reorganization of climate was observed between the Early and Late Oligocene. The climate anomalies between the Oligocene and present indicate that geographic changes (e.g. retreat of the Paratethys Sea) played an important role in shaping the climate pattern of Eurasia. By comparing the fossil data to a range of different HadCM3L model simulations of the Oligocene with differing boundary conditions (e.g. CO<sub>2</sub> and topography), we demonstrate similar large-scale climate spatial patterns between models and fossil data, however, models simulated much higher temperature seasonality (lower simulated winter temperatures and higher simulated summer temperatures) in Eurasia. Mean annual temperature analysis indicates that simulations with 560 and 1120 ppmv CO<sub>2</sub> matched better with fossil data when compared to other simulations, depending on the topography. These results provide some constraints that should be considered for future paleoclimate modeling.

**Keywords:** Oligocene, Eurasia, paleoclimate, fossil, simulation

## 1. Introduction

The Oligocene (33.9–23.03 Ma) is an important epoch of the Cenozoic because it marks an early modern ‘icehouse’ climate with the formation of large ice sheets in the Antarctic (Pälike et al., 2006; Zanzari et al., 2007). Major advances in understanding the Oligocene climate have come through the use of geochemical proxies from deep-sea sediments (Zachos et al.,

2001; Pälike et al., 2006; Zachos et al., 2008), fossil proxies from terrestrial sediments (Mosbrugger et al., 2005; Popova et al., 2012), and paleoclimate modelling results (Ramstein et al., 1997; Eldrett et al., 2009). Proxies and modelling results suggest that the Oligocene climate was generally warmer and more humid than the present day (Pekar and Christie-Blick, 2008). However, reconstructions from a variety of proxies and models show there are many uncertainties yet to be resolved especially in the higher latitudes of the Northern Hemisphere (Zanazzi et al., 2007; Zachos et al., 2008; Liu et al., 2009). The inconsistencies from different proxies and models thus question the validation of the Oligocene climate reconstructions and constrain our understanding of Oligocene climate forcings. Therefore, a comprehensive study of Oligocene climate in time and space is required to help resolve these disparities and to explore the Oligocene climate forcings.

Abrupt cooling at the Eocene-Oligocene transition (EOT) and the forcings exerted on the climate are key topics of interest (Liu et al., 2009). Modelling and isotope studies suggest that Greenhouse Gas (GHG) decline may have contributed to the EOT climate cooling (Pagani et al., 2005; Pearson et al., 2009). Meanwhile, geological evidence indicates that tectonic modification can also have major effects on climate (Ramstein et al., 1997; Steininger and Wessely, 2000). From the Oligocene to the Neogene period, significant tectonic and geographic changes occurred throughout Eurasia which may have had major effects on the climatic patterns throughout the continent (Seton et al., 2012). The Paratethys Sea became isolated from the Tethys Sea from the EOT onwards and retreated progressively during the Miocene modifying existing oceanic and atmospheric climate patterns in Europe and central Eurasia (Ramstein et al., 1997; Steininger and Wessely, 2000). In eastern Asia, the uplift of the Tibetan Plateau may have intensified the Asian monsoon system and may have contributed to global cooling during the Cenozoic, which is more evidenced at the EOT (Dupont-Nivet et al., 2007). Other geographic changes, such as opening of the Drake Passage

and Tasman Sea gateways and the glaciation of Antarctica may also have impacts on the global climate system effecting the northern higher latitude area through teleconnection (Scher et al., 2015). Therefore, to better understand Cenozoic climate change, it is crucial to explore Oligocene climate patterns in Eurasia and identify the climate forcings behind it.

Fossil data can provide important information for continental paleoclimate reconstruction (Mosbrugger et al., 2005). For instance, analysis of Bulgarian flora has suggested that southeastern Europe experienced warm and moderately humid subtropical climatic conditions during the Oligocene (Bozukov et al., 2009). In central Europe, fossil data indicate lower temperature in the Oligocene compared to the warm Eocene climate (Mosbrugger et al., 2005). The carpological records in Siberia and the Russian Far East show that warm and wet climate conditions prevailed in this area during the Oligocene (Popova et al., 2012). In northeast China, fossil data indicate a humid climate with distinct seasonality during the Oligocene (Guo and Zhang, 2001; Guo et al., 2008). These reconstructions demonstrate a subtropical, moderately humid climate during the Oligocene, generally above freezing in the winter with low seasonality in mid-high latitudes in Eurasia (Utescher et al., 2000; Mosbrugger et al., 2005; Bozukov et al., 2009; Erdei et al., 2012; Popova et al., 2012).

Climate modelling has been widely used to explore Paleogene climate change (Ramstein et al., 1997; Eldrett et al., 2009; Huber and Caballero, 2011). The simulations show that modelled Eocene greenhouse climate conditions generally yield larger temperature seasonality in the higher latitudes compared to proxies such as fossils, isotopes and biomarkers (Eldrett et al., 2009; Sluijs et al., 2009; Huber and Caballero, 2011). As the Earth entered the Oligocene icehouse phase, coeval with global cooling, winter temperature decreased dramatically in the Northern Hemisphere, leading to greater temperature seasonality (Zanazzi et al., 2007; Eldrett et al., 2009). Models also show relatively warm winters and high precipitation in Eurasia, suggesting a maritime type climate during the

Oligocene (Ramstein et al., 1997). Although these studies have improved our understanding of the Oligocene climate, there has been little in the way of direct Oligocene model-proxy comparison on a continental scale. Single basin analysis can only be indicative of local scale processes and not necessarily continental/global scale processes. Therefore, large continental model-proxy comparisons can provide a general view of the climate pattern and help us to better understand the climate forcings.

In this study, we have compiled a database of 149 Oligocene macro-fossil floras across the mid-high latitudes of Eurasia. We quantitatively reconstructed paleoclimate data using the Coexistence Approach (CA, Mosbrugger and Utescher, 1997) for 114 floras, and combined this with 35 published paleoclimate records (Popova et al., 2012), to explore both temporal and spatial climate variability through Eurasia in the Oligocene. A comparison against a set of paleoclimate model simulations with differing boundary conditions (CO<sub>2</sub> and paleogeography) using the UK Met Office GCM (General Circulation Model), HadCM3L is then presented (Valdes et al, 2017), followed by discussion of the potential driving factors leading to the observed changes in climate shown in the fossil record.

## **2. Materials and Methods**

### *2.1 Paleoflora data*

The 149 Oligocene paleofloras containing their locations were compiled for the mid-high latitudes of Eurasia (Appendix 1), including 114 leaf or wood floras and carpofloras in the Cenozoic Angiosperm Database (Xing et al., 2016), and 35 carpofloras from Siberia and the Russian Far East (Popova et al., 2012). These fossil floras are distributed in three regions: Europe, central Eurasia and eastern Asia. These floras were assigned into the Early Oligocene

(Rupelian, 33.9–28.1 Ma) and the Late Oligocene (Chattian, 28.1–23.03 Ma) based on the geological ages derived from original papers or latest revised publications.

## 2.2 Methods

The Coexistence Approach (CA, Mosbrugger and Utescher, 1997) was used to calculate paleoclimate data for 114 fossil floras, and other paleoclimate data derived from 35 carpofloras from Siberia and the Russian Far East (Popova et al., 2012). The CA has been widely applied for quantitative terrestrial climate reconstructions of the Cenozoic (Mosbrugger and Utescher, 1997; Utescher et al., 2014). Uncertainty in the CA still remains due to different factors, including unclear relationship between fossil and nearest living relative (NLR) taxa, different distribution and climate scope between fossil and living taxa, as well as uncertainty of climate threshold for NLR taxa. However, through continued updating of the climate database integrated in the CA and careful consideration of the results, this uncertainty can be lessened to yield comparable paleoclimate data through time and space (Utescher et al., 2014). The CA uses the climatic ranges of the nearest living relatives (NLRs) of all recognized taxa with known botanical affinity in a fossil flora to determine the climatic range in which the majority of the flora could coexist (Mosbrugger and Utescher, 1997; Utescher et al., 2014). NLRs (and associated climate parameters) were defined according to the original publications and PALAEOFLORA database (<http://www.palaeoflora.de/>). The paleoclimate was calculated based on generic level if applicable. For extinct genera with unclear affinities we use the family level. Problematic taxa were excluded from the analysis, e.g., monotypic or relict taxa such as *Cathaya*, *Metasequoia*, *Sequoia*, *Glyptostrobus*, and *Comptonia*, which have been distributed in large areas in geological times compared to the present day, thus could generate climate bias if included in the CA analysis (Utescher et al.,

2014). The program ClimStat was used to derive 7 quantitative climatic variables, i) mean annual temperature (MAT, °C), ii) mean temperature of the coldest month (CMT, °C), iii) mean temperature of the warmest month (WMT, °C), iv) mean annual precipitation (MAP, mm), v) mean precipitation of the driest month (DryMP, mm), vi) mean precipitation of the wettest month (WetMP, mm); and vii) mean precipitation of the warmest month (WarmMP, mm). The WarmMP data were not used for further analysis but shown in the supplementary information to provide more details of the reconstructed climate.

Climate anomalies between the Oligocene and present were analyzed to explore the climate change and climate forcings. The observed present climate parameters were calculated for each locality based on paleo-coordinate. The paleo-coordinates of fossil localities were generated using the Getech Group plc. plate model (Lunt et al., 2016). Climate data for each fossil site were extracted using the Bioclimatic envelope model in the R package ‘Dismo’ based on paleo-coordinates for each fossil locality. The present climate data were derived from the WorldClim database (<http://www.worldclim.org>, 10 minutes in resolution). The mean value of 20 km data (approximately 10 minutes resolution) were extracted.

The fossil results were then compared with results from the HadCM3L climate models (Valdes et al, 2017, with a resolution of 3.75°×2.5° longitude and latitude), including some new simulations and some described in previous publications (Kennedy et al., 2015; Lunt et al., 2016) from Bristol Research Initiative for the Dynamic Global Environment (BRIDGE). These simulations were set up with different conditions, including different CO<sub>2</sub> level (280ppmv, 560 ppmv, 840 ppmv, and 1120 ppmv), and different paleogeographic reconstructions (provided by Robertsons and Getech Group Plc.). The differences were calculated by simulation data minus fossil data for each locality at the correct paleo-coordinates for the Oligocene. Different regions have different numbers of fossil localities



thus could yield regional bias. In order to reduce this regional bias, the mean values of three regions were calculated and then the mean values of the entire study area were derived from these three-regional means. The modelled temperature parameters were corrected to mean sea level, because most of the fossil plants are found from lacustrine or fluviatile sediments, indicating these fossil floras are very likely preserved in lower altitude basins and valleys, thus closer resembling sea level climate. The best matched simulations from the Rupelian and the Chattian were chosen to visualize the disparity between fossil and modelling results, which were determined by the lowest anomaly in mean value of MAT between model and fossil data.

## 3 Results

### 3.1 Overall Oligocene climate type in Eurasia

The range of reconstructed MAT, CMT and WMT in Eurasia were 5.4–25.5 °C, -6.9–21.4 °C and 18.9–29.3 °C respectively, while MAP, DryMP, WetMP and WarmMP were 338–2453 mm, 2–180 mm, 84–340 mm and 19–227 mm respectively (Appendix 1). The reconstructed climate variables in the majority of sites in Eurasia were characterised by a warm and humid summer and relatively mild or cool winter. Overall, the reconstructed Oligocene climate in most of Eurasia resembled a subtropical humid climate (i.e., Cfa and Cwa climate according to the Köppen climate classification; Peel et al., 2007) with distinctive seasonality dominating most of the area in Eurasia.

### 3.2 Temperature variability

The reconstructed Oligocene temperatures (median values of MAT, CMT, and WMT) show prominent regional spatial variability (Fig. 1 and Fig. S1). Europe was the warmest region with a range of MAT between 9.4 °C and 25.5 °C, central Eurasia was the coldest area with a range of MAT between 5.4 °C and 21.3 °C, and eastern Asia had a moderate temperature with a range of MAT between 9.1 °C and 23.6 °C (Appendix 1). The warmest region in Eurasia was in the southern part of Central Europe around the Paratethys Sea (Fig. 1). For instance, Nagysáp flora in Hungary (Hably, 1989) and Trbovlje flora in Slovenia (Erdei et al., 2012) with MAT of 20.6–25.0 °C and 17.2–25.5 °C respectively, were significantly warmer than others (Appendix 1).

Temperature regimes between the Early Oligocene and Late Oligocene were similar, but with minor differences in different regions (Fig. 1, Fig. S1 and Appendix 1). Temperatures increased slightly from the Early to Late Oligocene in central Eurasia and eastern Asia (Fig. 1). The median MAT, CMT and WMT in central Eurasia increased from 14.1 to 15 °C, 3.2 to 3.9 °C, and 23.3 to 24.9 °C respectively (Fig. S1 and Appendix 1). In eastern Asia, the median MAT and CMT increased from 15.1 to 15.5 °C and 3.6 to 5.8 °C respectively, and WMT remained constant value of 24.9 °C (Fig. S1 and Appendix 1). However, in Europe temperature decreased slightly (Fig. 1) with the median MAT, CMT and WMT decreasing from 19.2 to 18.5 °C, 9.2 to 9.0 °C, and 26.4 to 25.9 °C respectively (Fig. S1 and Appendix 1).

Fig. 1.

### *3.3 Precipitation variability*

The reconstructed precipitation patterns for the Oligocene (Fig. 2 and Fig. S2) indicate large spatial variations. Highest MAP and WetMP occurred in Europe and the lowest

occurred in central Eurasia: the range of MAP in Europe was 505–2453 mm, central Eurasia 338–1613 mm, and eastern Asia 470–1812 mm (Appendix 1). DryMP shows that Europe was slightly drier than the other two regions (Appendix 1).

The results demonstrate that precipitation patterns changed slightly from the Early to Late Oligocene, but with spatial disparities (Fig. 2, Fig. S2 and Appendix 1). MAP and WetMP decreased in Europe, but increased in both of the other regions (Fig. 2, Fig. S2 and Appendix 1); DryMP increased a little in Europe and central Eurasia but decreased slightly in eastern Asia from the Early Oligocene to the Late Oligocene (Fig. 2, Fig. S2 and Appendix 1).

Fig. 2

### *3.4 Climate anomalies between the Oligocene and present*

The Oligocene temperatures show generally warmer conditions compared to the present day in the studied regions, with the exception of some sites in eastern Asia and around the Paratethys Sea, which display slightly lower WMT values in the Oligocene (Figs. 3A–C). Temperature anomalies in central Eurasia and summer temperature anomalies (WMT) in Europe increased with distance from the Paratethys Sea (Figs. 3A–C). The largest MAT and CMT anomalies were in central Eurasia, especially in the northeast of central Eurasia (Figs. 3A and B). The largest WMT anomalies were found in Europe especially in western and central Europe (Fig. 3C). In eastern Asia, temperature anomalies increased from south to north.

Fig. 3.

Our results indicate that during the Oligocene, conditions were generally much wetter than the present day, but different regions show obvious spatial variability (Figs. 3D–F). Europe generally had lower DryMP anomalies but higher WetMP anomalies compare to other regions (Figs. 3E and F). In central Eurasia, regions around the Paratethys Sea show higher WetMP anomalies compared to the further inland regions (Fig. 3F). DryMP anomalies in central Eurasia were much higher than other regions (Fig. 3E). In eastern Asia, sites to the south were drier than they are today especially in summer, while most of sites in north and in central China were much wetter than present (Figs. 3D–F).

### *3.5 Model–data comparison: different simulations*

#### *3.5.1 The Rupelian stage*

Thirty-five modelling results for the Rupelian were compared with fossil data (Fig. 4). A detailed description of the modelling setup for both the Rupelian and the Chattian is included in the Appendix 2. Our results show that the Getech Group Plc. simulations generated lower MAT compared to fossil data at CO<sub>2</sub> levels of 560 ppmv, however at CO<sub>2</sub> levels of 1120 ppmv they show near exact agreement with the data. In contrast, Robertsons simulations predicted similar MAT compared to the CA derived fossil records when assigned with CO<sub>2</sub> levels of 560 ppmv (Fig. 4). The most prominent differences between models and fossil data were in CMT and WMT, indicating this suite of simulations has higher temperature seasonality, suggesting that HadCM3L has a stronger seasonal cycle than indicated by the fossil record (Fig. 4). Fig. 4 indicates that simulations at CO<sub>2</sub> levels of 560, 840 and 1120 ppmv better matched with fossil data for MAT and CMT, while CO<sub>2</sub> level at 560 ppmv achieved better results for WMT. For precipitation variables, the Getech Group Plc.

simulations matched well with fossil data, while the Robertsons simulations generated slightly lower values compared to fossil data especially for DryMP. Different CO<sub>2</sub> levels show no significant impacts on precipitation variables.

Fig. 4.

### 3.5.2 The Chattian stage

Fourteen climate simulations for the Chattian were compared to the fossil data (Fig. 5 and Appendix 2). Fig. 5 indicates all the simulations generated lower MAT compared to the fossil data, except for one Robertsons simulation ('tedjp') with higher CO<sub>2</sub> level (1120 ppmv) which matched well. The Robertsons models matched better with fossil results compare to the Getech Group Plc. simulations when considering MAT. All the simulations show significantly higher temperature seasonality (lower CMT and higher WMT) than fossil data. For precipitation, all simulations were too dry. The precipitation disparities were not as significant as temperature when the different scales for these variables are considered. As with the Rupelian, precipitation was less sensitive than temperature to changes in CO<sub>2</sub>.

Fig. 5.

### 3.6 Model–data comparison: Spatial variability

Determined by the mean annual temperature (MAT) differences between model and fossil data, the best matched simulations 'tecqn1' (Rupelian) and 'tedjp' (Chattian) were chosen to visualize the disparity between fossil and modelling results (Figs.4–5, Appendix 2). Fig. 6 and Fig. 7 show similar large-scale spatial patterns between the fossil reconstructions and

simulations for the Oligocene temperature variables (Europe was the warmest region, and central Eurasia was the coldest region; the lower latitude regions generally had higher MAT compared to the higher latitudes). However, there were some disparities between the simulations and fossil data. In particular CMT and WMT indicate lower and higher values than those of the fossil reconstructions for both the Rupelian and the Chattian. This disparity was particularly evident in the higher latitudes of central Eurasia, where boreal WMT in both simulations were warmer than that of fossil records. Overall, in agreement with the analysis in the previous section on the global scale, the models yielded a larger temperature seasonality than indicated by the fossil record. Precipitation spatial patterns were similar between the fossil data and simulations (e.g, central Eurasia is the driest while eastern Europe is the wettest region). However, in some regions precipitation in the simulations was lower than that of fossil record, in particular for boreal summer precipitation in central Eurasia (Figs. 6 and 7).

Fig. 6.

Fig. 7

## 4. Discussion

### *4.1 A subtropical humid climate*

The reconstructed Oligocene climate in both the proxies and models indicates that a humid subtropical climate with a distinct seasonal cycle prevailed across Eurasia, generally consistent with most previous climate reconstructions (Utescher et al., 2000; Mosbrugger et

al., 2005; Uhl et al., 2007; Erdei et al., 2012; Popova et al., 2012; Quan et al., 2012). Many fossil floras show the majority elements are evergreen and deciduous taxa (Kvacek and Walther, 2001; Erdei and Bruch, 2004; Erdei et al., 2012), as well as mesophytic forest mixed with conifers (Akhmetiev et al., 2009; Erdei et al., 2012) in mid-high latitudes of Eurasia, implying a warm-temperate or subtropical humid climate with distinct seasons existed in these regions (Kvacek and Walther, 2001; Erdei and Bruch, 2004; Erdei et al., 2012). Some floras contain high proportion of thermophilic taxa or deciduous elements, mostly from higher latitudes of Eurasia, especially in Siberia and the Russian Far East (Kvacek and Walther, 2001; Akhmetiev et al., 2009; Bozukov et al., 2009; Erdei et al., 2012). Fossil evidence from eastern Asia indicates that temperate or warm temperate elements mainly occurred in this region, as well as many subtropical elements such as Rutaceae, Euphorbiaceae, Sapindaceae, Myrsinaceae, Apocynaceae and Boraginaceae, indicating a temperate to warm-temperate climate (Tanai and Uemura, 1991; Guo and Zhang, 2001; Popova et al., 2012; Quan et al., 2012). It should be noted that the humid subtropical climate is a definition including Cfa and Cwa (the coldest month average temperature above 0 °C and warmest average temperature above 22 °C) according to Köppen climate classification (Peel et al., 2007; also refer to [https://www.weather.gov/jetstream/climate\\_max](https://www.weather.gov/jetstream/climate_max)). Therefore, the temperate to warm-temperate climate discussed above can broadly be included in Cfa and Cwa, i.e., humid subtropical climate.

#### *4.2 Climate shift from the Early to Late Oligocene*

Different studies have shown inconsistent results for climate changes from the Early to Late Oligocene (Erdei and Bruch, 2004; Mosbrugger et al., 2005; Popova et al., 2012; Quan et al., 2012). The macro-floras in Hungary indicate that the Late Oligocene had lower MAT

and CMT compared to the Early Oligocene (Erdei and Bruch, 2004). In central Europe, fossil data reveal significant warming during the uppermost part of the Late Oligocene, coinciding with the Late Oligocene warming events (Mosbrugger et al., 2005). In western Siberia, WMT increased slightly from the Early to Late Oligocene, but CMT decreased a little (Popova et al., 2012). While in China, the leaf fossil and pollen data indicate a cooling trend during the Late Oligocene, which may be linked to Tibetan uplift and monsoon evolution (Quan et al., 2012). Taken together with this evidence, our results suggest that the differences between the Early and Late Oligocene show strong spatial heterogeneity patterns. Modelling results support the fossil data, suggesting that there is little change in global climate between the Early and Late Oligocene. However, the modelling data do display diverse spatial variability (Fig. 6 and Fig. 7), likely a result of perturbations in geographic and orographic forcing through the Oligocene. Overall, the fossil data suggest that any signals are indicative of local/regional change and not that of a global signal, corroborated by our suite of GCM simulations of the Early and Late Oligocene.

#### *4.3 The influence of paleogeography on climate patterns*

Spatial patterns presented in the data for Europe and central Eurasia imply that the retreat of the Paratethys Sea may have played an important role in the Oligocene climate regime. During most of the Oligocene, the Paratethys Sea covered large areas of the central Eurasia, thus the asymmetric heating of land and sea may lead to the warmer and humid winter climate in central Eurasia (Ramstein et al., 1997). With the retreat of the Paratethys Sea, the climate of central Eurasia became colder and dryer resulting in a typical continental climate which is consistent with modelling results (Ramstein et al., 1997). This highlights the major role of the Paratethys Sea as a thermal regulator of the Oligocene climate in Eurasia. The



Paratethys is able to facilitate the northerly advancement of sub-tropical warm moist air masses into central Asia during the boreal summer (Fig. 8B) allowing a humid subtropical climate to be sustained in more northerly latitudes that would have otherwise been located further south.

Fig. 8 shows the simulated wind intensity (m/s) and trajectories at 850 hPa during the Oligocene. During the Rupelian, the results indicate that westerlies prevailed in winter at mid-high latitudes (Fig. 8A). In Asia in the boreal winter the lower elevations of Tibetan and Mongolian plateaus compared to the present day favoured the generation of more intense westerly winds over the Eurasian continent allowing greater moisture supply into central Eurasia (Fig. 8A). The central Asia high-pressure system was weaker than present and may have been shifted south to eastern China (Ramstein et al., 1997; Licht et al., 2016). Therefore, winter was much warmer and more humid in central Eurasia during the Oligocene. Recent meteorological data show remarkable weakening of the Siberian High in recent years, leading to warm winter and higher mean annual temperature in higher latitudes of Eurasia, further supporting our results (Gong and Ho, 2002).

Fig. 8

The atmospheric circulation changes in Eurasia not only influenced the climate of central Eurasia but also influenced the monsoon system in eastern Asia (Zhang et al., 2007; Spicer, 2017). Previous studies based on various proxies suggest that the summer monsoon in East Asia intensified through the Cenozoic due to the uplift of Tibetan Plateau and other plate motions (Ramstein et al., 1997; Sun et al., 2010). Numerical modelling demonstrates southwest prevailing wind intensified in summer, caused by the Tibetan Plateau uplift and the Paratethys retreat, providing large amount of water and increased precipitation in the

monsoon areas in eastern Asia (Zhang et al., 2007). Sensitivity experiments also suggest that when the Qinghai–Tibetan Plateau (QTP) is set flat (0 m), the South and Southeast Asian monsoons still prevail (Liu et al., 2015). Some other fossil data also suggest that the Asian monsoon established during the early Cenozoic period (Spicer et al., 2016, 2017). Our results, combined with fossil and model data, indicate distinct precipitation seasonality in eastern Asia, suggesting that monsoonal climate existed in this region. However, our results show that summer precipitation during the Oligocene is lower than the present day in southern parts of eastern Asia, which currently is remarkably affected by the Asian summer monsoon, indicating that the summer monsoon in these regions may not have been as intense as the present day during the Oligocene.

The winter monsoon in eastern Asia was dramatically different in the Oligocene compared to the present day (Sun et al., 2010), and consequently influenced winter precipitation (Sun et al., 2010). The winter monsoon which is dynamically linked to the strength and position of the high pressure centre over the Siberian–Mongolian region normally yields a dry winter (Wu and Chan, 1997). Therefore, the higher precipitation in winter may indicate lower winter monsoon strength in east Asia. As discussed above, the central Asia high-pressure system was weaker than present, thus can result in a weaker winter monsoon in eastern Asia (Zhang et al., 2007). In addition, penetration of moisture from the Paratethys Sea into central Asia also could lead to a more humid winter. This is consistent with our results that the Oligocene was much wetter than today during winter, indicating a weaker winter monsoon in northeastern Asia (Zhang et al., 2007; Clift et al., 2008; Sun et al., 2010).

#### *4.4 Fossil results versus models*

Reconstructed CO<sub>2</sub> proxy data can yield a large range in CO<sub>2</sub> concentrations during the Oligocene (Beerling and Royer, 2011; Pagani et al., 2005), but the majority of data suggests that atmospheric CO<sub>2</sub> concentrations significantly dropped during the Oligocene, reaching moderate-to-low levels (280–840 ppmv) compared to the pre-industrial era (Beerling and Royer, 2011; Pagani et al., 2005; Roth-Nebelsick et al., 2014; Zhang et al., 2013). Our results show sensitivity to CO<sub>2</sub> concentrations when considering simulated temperature comparisons with fossil data. CO<sub>2</sub> levels of 560 ppmv and 1120 ppmv matched better with the Rupelian fossil results for Robertsons and Getech Group Plc. simulations respectively, while for the Chattian, only one Robertsons simulation with 1120 ppmv was comparable with the fossil data. These simulations are broadly consistent with published CO<sub>2</sub> results, especially for Robertsons simulations of the Rupelian period. Getech Group Plc. simulations generally need higher CO<sub>2</sub> level to match better with fossil data, indicating there could potentially be some orographic or model spin-up impacts on simulated temperatures which need consider further exploration.

The mean values from all the simulations broadly matched well with fossil data, mainly because mean values generally reduced the range in the data. Consequently, multi-simulation means with perturbed boundary conditions can produce robust results compared to a single model (Knutti and Sedláček, 2013.). Nevertheless, substantial uncertainty remains in the use of multiple simulation means, in particularly on a process-based level. Quantitative evaluation of this uncertainty should be considered in further work to understand the differences between simulations.

Both fossil data and climate models demonstrate a similar spatial pattern on a broad continental scale, with central Eurasia being the coldest and driest region, and Europe and eastern Asia being much warmer and more humid, implying these two results are consistent and comparable. However, there are distinct differences between the models and fossil data;

in particular, there is prominent disparity between both fossil and modeled seasonality during the Oligocene with the latter indicating a much greater seasonal range in temperature. These differences can be derived from the uncertainties from both fossil reconstruction and the modeling approach. The CA normally represents the climate of a particular fossil flora, however, it assumes that fossil taxa has a similar climate envelope as their NLRs. Thus, there is potential to generate large errors when applied to early geological ages (Utescher et al., 2014). Fossil taxa may have different climate scope (or thresholds) compared to modern taxa because of evolution, thus the bias may not be the same for different climate parameters. For example, some taxa may be widely distributed in the geological past but now are restricted to specific areas, therefore the range from CMT and/or WMT may be different than in the present day, yet the equivalent MAT can still be similar to the present day. In addition, the unclear identification of some NLR taxa and modern taxa climate data could also contribute to uncertainties (Utescher et al., 2014).

Climate models can produce uncertainties due to the prescribed parameters and various data inputs, some of which are poorly constrained and thus they could have large effects on the paleoclimate modelling results (Valdes, 2000). There have been a number of studies which have compared fossil, isotope and biomarker results to those of model simulations, indicating models could yield significantly lower winter temperatures and produce higher temperature seasonality at higher latitudes, during past warm periods such as the Eocene and Cretaceous (Herman and Spicer, 1996; Eldrett et al., 2009; Sluijs et al., 2009; Huber and Caballero, 2011). CO<sub>2</sub> concentration is the most important and unfortunately unconstrained factor that can dramatically altered the modeling results (Anagnostou et al., 2016), although it has less effect on seasonality (Figs. 4 and 5). As is shown in the modeling results, when set up with mid-high CO<sub>2</sub> levels (560–1120 ppmv) for the Rupelian, models give a good match the fossil data for MAT, but the temperature seasonality remains consistent regardless of CO<sub>2</sub>

level (Figs. 4 and 5). However, atmospheric CO<sub>2</sub> reconstructions for the Oligocene are limited and different proxies display large uncertainties (Pearson et al., 2009; Zhang et al., 2013), thus limiting the validation of modelling results. Geographic and orographic features may dramatically affect the regional climate by altering the atmospheric and oceanic circulation and the land surface-atmosphere interaction (Clark et al., 2001). Therefore, different paleogeographic and orographic settings can generate differing sensitivities as was highlighted in our results section, comparing Getech Group Plc. and Robertsons simulations. Climate-vegetation interactions could also contribute to the disparities. The climate model interactively predicts vegetation cover so does include vegetation climate feedbacks but may not represent them well. Models at the Eocene/Oligocene boundary suggest that temperature and the Antarctic ice sheet are highly sensitive to vegetation types (Liakka et al., 2014). Some of the simulations also included alternative Antarctic ice sheet configurations but the climatic differences in the Northern Hemisphere were small and did not change the model data comparison suggesting an insensitivity to interhemispheric teleconnections resulting from different ice sheet configurations on the vegetation and climate of Eurasia in both proxies and models. Other important factors such as the ozone layers, clouds and soil data can also contribute some uncertainties (Sluijs et al., 2009).

Overall, it is hard to say whether the CA results from fossil floras are able to adequately resolve the climate variability which can lead to extremes in climate that could be recorded in the fossil data. Interannual, interdecadal and/or intercentennial variability could bias the result and comparison. However, when considering other proxies and model results (e.g., Herman and Spicer, 1996; Eldrett et al., 2009; Sluijs et al., 2009; Huber and Caballero, 2011), we suggest that some parameters or mechanisms embedded in the models may profoundly increase higher latitude temperature seasonality in Eurasia. Possible factors responsible for this include: ground cover (different vegetation), clouds, topographic representation, ocean

circulation, equator-polar energy transport, and even different resolution of the model. Refined data and sensitivity experiments should be considered for further studies, and the feedbacks between climate and key factors may provide clues for future climate predictions.

## 5. Conclusion

Our study based on a large dataset of fossil floras provides a comprehensive picture of the continental climate during the Oligocene. The reconstructed paleoclimates indicate a typical humid subtropical climate with distinct seasonality during the Oligocene. Our results show a spatial heterogeneity of climate change patterns between the Early and Late Oligocene. The anomalies of the Oligocene compared to the present suggest that the plate motion and land-sea distribution caused by the Paratethys Sea retreat and Tibetan Plateau uplift may have played important role in shaping the climate of Eurasia since at least the Oligocene. We compared the fossil data with a range of different HadCM3L simulations of the Oligocene with differing boundary conditions. Our results suggest that fossil and modelling results are generally spatial consistent but have some distinct disparities. Our findings, in agreement with other studies from the Eocene and Oligocene, suggest that models generate higher temperature seasonality and lower precipitation than fossil proxy reconstructions. Further analysis indicates that different CO<sub>2</sub> concentration and topographic representations of Eurasia may be responsible for the differences in the model-data comparisons. Middle to high CO<sub>2</sub> levels (560 and 1120 ppmv) and Robertsons simulations matched better with reconstructed temperatures from the fossil record than Getech Group Plc. simulations. Therefore, we suggest further sensitivity experiments should be conducted to explain the disparities between model and proxies in higher latitude regions.

## Acknowledgements

This study was supported by the NSFC-RCUK NERC joint project (No. 41661134049), the grant of Natural Environment Research Council (No. NE/P013805/1), National Natural Science Foundation of China (No. 41772026, 41372035, and U1502231), the Pioneer Hundred Talents Program of the Chinese Academy of Sciences (No. 2016-062 to Y.W. Xing), the Foundation of the State Key Laboratory of Paleobiology and Stratigraphy, Nanjing Institute of Geology and Palaeontology, Chinese Academy of Sciences (No. 153107), the CAS 135 program (XTBG-F01), NERC grant (No. NE/K014757/1; Cretaceous-Paleocene-Eocene: Exploring Climate and Climate Sensitivity) and NERC grant (NE/L002434/1). We thank Dr. Torsten Utescher and another anonymous reviewer for their many insightful comments and constructive suggestions. This work is part of the NECLIME (Neogene Climate Evolution of Eurasia) network.

## Appendices

## References

- Akhmetiev, M., Walther, H., Kvaček, Z., 2009. Mid-latitude Palaeogene floras of Eurasia bound to volcanic settings and palaeoclimatic events—experience obtained from the Far East of Russia (Sikhote-Alin') and Central Europe (Bohemian Massif). *Acta Musei Nationalis Pragae, Series B Historia Naturalis* 65, 61-129.
- Anagnostou, E., John, E.H., Edgar, K.M., Foster, G.L., Ridgwell, A., Inglis, G.N., Pancost, R.D., Lunt, D.J., Pearson, P.N., 2016. Changing atmospheric CO<sub>2</sub> concentration was the primary driver of early Cenozoic climate. *Nature* 533, 380-384.

- Beerling, D.J., Royer, D.L., 2011. Convergent Cenozoic CO<sub>2</sub> history. *Nature Geoscience* 4, 418.
- Bozukov, V., Utescher, T., Ivanov, D., 2009. Late Eocene to early Miocene climate and vegetation of Bulgaria. *Review of Palaeobotany and Palynology* 153, 360-374.
- Clark, D.B., Xue, Y., Harding, R.J., Valdes, P.J., 2001. Modeling the impact of land surface degradation on the climate of tropical North Africa. *Journal of Climate* 14, 1809-1822.
- Clift, P.D., Hodges, K.V., Heslop, D., Hannigan, R., Van Long, H., Calves, G., 2008. Correlation of Himalayan exhumation rates and Asian monsoon intensity. *Nature Geoscience* 1, 875-880.
- Dupont-Nivet, G., Krijgsman, W., Langereis, C.G., Abels, H.A., Dai, S., Fang, X.M., 2007. Tibetan plateau aridification linked to global cooling at the Eocene-Oligocene transition. *Nature* 445, 635-638.
- Eldrett, J.S., Greenwood, D.R., Harding, I.C., Huber, M., 2009. Increased seasonality through the Eocene to Oligocene transition in northern high latitudes. *Nature* 459, 969-973.
- Erdei, B., Bruch, A., 2004. A climate analysis of Late Oligocene (Egerian) macrofloras from Hungary. *Studia Botanica Hungarica* 34, 5-23.
- Erdei, B., Utescher, T., Hably, L., Tamas, J., Roth-Nebelsick, A., Grein, M., 2012. Early Oligocene continental climate of the Palaeogene Basin (Hungary and Slovenia) and the surrounding area. *Turkish Journal of Earth Sciences* 21, 153-186.
- Gong, D.Y., Ho, C.H., 2002. The Siberian High and climate change over middle to high latitude Asia. *Theoretical and Applied Climatology* 72, 1-9.
- Guo, S.Y., Zhang, G.F., 2001. Oligocene Sanhe flora in Longjing county of Jilin, northeast China. *Acta Palaeontologica Sinica* 41, 193-210.



- Guo, Z.T., Sun, B., Zhang, Z.S., Peng, S.Z., Xiao, G.Q., Ge, J.Y., Hao, Q.Z., Qiao, Y.S.,  
Liang, M.Y., Liu, J.F., 2008. A major reorganization of Asian climate by the early  
Miocene. *Climate of the Past* 4, 153-174.
- Hably, L., 1989. The Oligocene flora of Nagysap. *Fragm. Mineral. Palaeont* 14, 83-99.
- Herman, A.B., Spicer, R.A., 1996. Palaeobotanical evidence for a warm Cretaceous Arctic  
Ocean. *Nature* 380, 330-333.
- Huber, M., Caballero, R., 2011. The early Eocene equable climate problem revisited. *Climate  
of the Past* 7, 603.
- Kennedy, A., Farnsworth, A., Lunt, D., Lear, C.H., Markwick, P., 2015. Atmospheric and  
oceanic impacts of Antarctic glaciation across the Eocene–Oligocene transition. *Phil.  
Trans. R. Soc. A* 373, 20140419.
- Knutti, R., Sedláček, J., 2013. Robustness and uncertainties in the new CMIP5 climate model  
projections. *Nature Climate Change* 3, 369.
- Kvacek, Z., Walther, H., 2001. The Oligocene of Central Europe and the development of  
forest vegetation in space and time based on megafossils. *Palaeontographica  
Abteilung B*, 125-148.
- Liakka, J., Colleoni, F., Ahrens, B., Hickler, T., 2014. The impact of climate - vegetation  
interactions on the onset of the Antarctic ice sheet. *Geophysical Research Letters* 41,  
1269-1276.
- Licht, A., Dupont-Nivet, G., Pullen, A., Kapp, P., Abels, H., Lai, Z., Guo, Z., Abell, J.,  
Giesler, D., 2016. Resilience of the Asian atmospheric circulation shown by  
Paleogene dust provenance. *Nature communications* 7, 12390.
- Liu, Z.H., Pagani, M., Zinniker, D., DeConto, R., Huber, M., Brinkhuis, H., Shah, S.R.,  
Leckie, R.M., Pearson, A., 2009. Global cooling during the Eocene-Oligocene climate  
transition. *Science* 323, 1187-1190.

- 600 Lunt, D.J., Foster, G.L., O'Brien, C.L., Pancost, R.D., Robinson, S.A., 2016.  
601 Palaeogeographic controls on climate and proxy interpretation. *Climate of the Past* 12,  
602 1181.
- 603 Mosbrugger, V., Utescher, T., 1997. The coexistence approach—a method for quantitative  
604 reconstructions of Tertiary terrestrial palaeoclimate data using plant fossils.  
605 *Palaeogeography, Palaeoclimatology, Palaeoecology* 134, 61-86.
- 606 Mosbrugger, V., Utescher, T., Dilcher, D.L., 2005. Cenozoic continental climatic evolution  
607 of Central Europe. *Proc Natl Acad Sci U S A* 102, 14964.
- 608 Pagani, M., Zachos, J.C., Freeman, K.H., Tippie, B., Bohaty, S., 2005. Marked decline in  
609 atmospheric carbon dioxide concentrations during the Paleogene. *Science* 309, 600-  
610 603.
- 611 Pälike, H., Norris, R.D., Herrle, J.O., Wilson, P.A., Coxall, H.K., Lear, C.H., Shackleton,  
612 N.J., Tripathi, A.K., Wade, B.S., 2006. The heartbeat of the Oligocene climate system.  
613 *science* 314, 1894-1898.
- 614 Pearson, P.N., Foster, G.L., Wade, B.S., 2009. Atmospheric carbon dioxide through the  
615 Eocene–Oligocene climate transition. *Nature* 461, 1110-1113.
- 616 Peel, M.C., Finlayson, B.L., McMahon, T.A., 2007. Updated world map of the Köppen-  
617 Geiger climate classification. *Hydrology and Earth System Sciences Discussions* 4,  
618 439-473.
- 619 Pekar, S.F., Christie-Blick, N., 2008. Resolving apparent conflicts between oceanographic  
620 and Antarctic climate records and evidence for a decrease in pCO<sub>2</sub> during the  
621 Oligocene through early Miocene (34–16 Ma). *Palaeogeography, Palaeoclimatology,*  
622 *Palaeoecology* 260, 41-49.

- Popova, S., Utescher, T., Gromyko, D., Bruch, A., Mosbrugger, V., 2012. Palaeoclimate evolution in Siberia and the Russian Far East from the Oligocene to Pliocene—evidence from fruit and seed floras. *Turkish Journal of Earth Sciences* 21, 315-334.
- Quan, C., Liu, Y.-S., Utescher, T., 2012. Paleogene temperature gradient, seasonal variation and climate evolution of northeast China. *Palaeogeography, Palaeoclimatology, Palaeoecology* 313–314, 150-161.
- Ramstein, G., Fluteau, F., Besse, J., Joussaume, S., 1997. Effect of orogeny, plate motion and land-sea distribution on Eurasian climate change over the past 30 million years. *Nature* 386, 788-795.
- Roth-Nebelsick, A., Oehm, C., Grein, M., Utescher, T., Kunzmann, L., Friedrich, J.P., Konrad, W., 2014. Stomatal density and index data of *Platanus neptuni* leaf fossils and their evaluation as a CO<sub>2</sub> proxy for the Oligocene. *Review of Palaeobotany and Palynology* 206, 1-9.
- Scher, H.D., Whittaker, J.M., Williams, S.E., Latimer, J.C., Kordesch, W.E., Delaney, M.L., 2015. Onset of Antarctic Circumpolar Current 30 million years ago as Tasmanian Gateway aligned with westerlies. *Nature* 523, 580.
- Seton, M., Müller, R.D., Zahirovic, S., Gaina, C., Torsvik, T., Shephard, G., Talsma, A., Gurnis, M., Turner, M., Maus, S., Chandler, M., 2012. Global continental and ocean basin reconstructions since 200 Ma. *Earth-Science Reviews* 113, 212-270.
- Sluijs, A., Schouten, S., Donders, T.H., Schoon, P.L., Röhl, U., Reichart, G.-J., Sangiorgi, F., Kim, J.H., Damsté, J.S.S., Brinkhuis, H., 2009. Warm and wet conditions in the Arctic region during Eocene Thermal Maximum 2. *Nature Geoscience* 2, 777-780.
- Spicer, R.A., 2017. Tibet, the Himalaya, Asian Monsoons and Biodiversity-In what ways are they related? *Plant Diversity* 39, 233-244.

- Spicer, R.A., Yang, J., Herman, A.B., Kodrul, T., Maslova, N., Spicer, T.E., Aleksandrova, G., Jin, J., 2016. Asian Eocene monsoons as revealed by leaf architectural signatures. *Earth and Planetary Science Letters* 449, 61-68.
- Spicer, R., Yang, J., Herman, A., Kodrul, T., Aleksandrova, G., Maslova, N., Spicer, T., Ding, L., Xu, Q., Shukla, A., 2017. Paleogene monsoons across India and South China: Drivers of biotic change. *Gondwana Research* 49, 350-363.
- Steininger, F.F., Wessely, G., 2000. From the Tethyan Ocean to the Paratethys Sea: Oligocene to Neogene stratigraphy, paleogeography and paleobiogeography of the circum-Mediterranean region and the Oligocene to Neogene Basin evolution in Austria. *Mitteilungen der Österreichischen Geologischen Gesellschaft* 92, 95-116.
- Sun, J.M., Ye, J., Wu, W.Y., Ni, X.J., Bi, S.D., Zhang, Z.Q., Liu, W.M., Meng, J., 2010. Late Oligocene–Miocene mid-latitude aridification and wind patterns in the Asian interior. *Geology* 38, 515-518.
- Tanai, T., Uemura, K., 1991. The Oligocene noda flora from the Yuya-wan area of the western end of Honshu, Japan. I. *Bulletin of the National Science Museum. Series C* 17, 57-80.
- Uhl, D., Klotz, S., Traiser, C., Thiel, C., Utescher, T., Kowalski, E., Dilcher, D.L., 2007. Cenozoic paleotemperatures and leaf physiognomy—a European perspective. *Palaeogeography, Palaeoclimatology, Palaeoecology* 248, 24-31.
- Utescher, T., Bruch, A.A., Erdei, B., François, L., Ivanov, D., Jacques, F.M.B., Kern, A.K., Liu, Y.S., Mosbrugger, V., Spicer, R.A., 2014. The Coexistence Approach—Theoretical background and practical considerations of using plant fossils for climate quantification. *Palaeogeography, Palaeoclimatology, Palaeoecology* 410, 58-73.
- Utescher, T., Mosbrugger, V., Ashraf, A.R., 2000. Terrestrial Climate Evolution in Northwest Germany Over the Last 25 Million Years. *PALAIOS* 15, 430-449.

- Valdes, P., 2000. Paleoclimate modeling, in: Mote, P., O'Neill, A. (Eds.), Numerical modeling of the global atmosphere in the climate system. NATO Science Series: Mathematical and Physical Sciences, pp. 465-488.
- Valdes, P., Armstrong, E., Badger, M., Bradshaw, C., Bragg, F., Crucifix, M., Davies-Barnard, T., Day, J., Farnsworth, A., Gordon, C., 2017. The BRIDGE HadCM3 family of climate models: HadCM3@ Bristol v1. 0, *Geosci. Model Dev.*, 10, 3715–3743.
- Wu, M., Chan, J.C., 1997. Upper-level features associated with winter monsoon surges over South China. *Monthly Weather Review* 125, 317-340.
- Xing, Y.W., Gandolfo, M.A., Onstein, R.E., Cantrill, D.J., Jacobs, B.F., Jordan, G.J., Lee, D.E., Popova, S., Srivastava, R., Su, T., 2016. Testing the Biases in the Rich Cenozoic Angiosperm Macrofossil Record. *International Journal of Plant Sciences* 177, 371-388.
- Zachos, J., Pagani, M., Sloan, L., Thomas, E., Billups, K., 2001. Trends, rhythms, and aberrations in global climate 65 Ma to present. *Science* 292, 686-693.
- Zachos, J.C., Dickens, G.R., Zeebe, R.E., 2008. An early Cenozoic perspective on greenhouse warming and carbon-cycle dynamics. *Nature* 451, 279-283.
- Zanazzi, A., Kohn, M.J., MacFadden, B.J., Terry, D.O., 2007. Large temperature drop across the Eocene–Oligocene transition in central North America. *Nature* 445, 639-642.
- Zhang, Y.G., Pagani, M., Liu, Z., Bohaty, S.M., DeConto, R., 2013. A 40-million-year history of atmospheric CO<sub>2</sub>. *Phil. Trans. R. Soc. A* 371, 20130096.
- Zhang, Z.S., Wang, H.J., Guo, Z.T., Jiang, D.B., 2007. What triggers the transition of palaeoenvironmental patterns in China, the Tibetan Plateau uplift or the Paratethys Sea retreat? *Palaeogeography, Palaeoclimatology, Palaeoecology* 245, 317-331.

**Figure Captions:**

**Fig. 1** Comparison of temperature (median values of MAT, CMT, WMT) patterns between the Early (left hand panels) and Late (right hand panels) Oligocene in Eurasia. Topography was derived from the Robertsons paleogeographic data. The grey color lines and dark thick lines on the map represent the present day and Oligocene land–water boundaries respectively.

**Fig. 2** Comparison of precipitation (median values of MAT, DryMP, WetMP) patterns between the Early (left hand panels) and the Late (right hand panels) Oligocene in Eurasia. The geographic map was derived from Robertsons paleogeographic data. The grey color lines and dark thick lines on the map represent the present day and Oligocene land–water boundaries respectively.

**Fig. 3** Climate anomalies of the Oligocene and the present day observations in Eurasia. The anomalies are calculated by Oligocene minus the present day for MAT (A), CMT (B), WMT (C), MAP (D), DryMP (E) and WetMP (F) respectively. The geographic map (31 Ma) was derived from Robertsons paleogeographic data. The grey color lines on the map represent the present land–water boundaries.

**Fig. 4** The differences between models and all fossil data for the Rupelian period. The Y axes refer to the differences between modelling results and the fossil climate data (mean value of model data minus fossil data) for MAT, CMT, WMT, MAP, DryMP and WetMP respectively. The X axes indicate different simulation names. Different bar colors indicate different CO<sub>2</sub> level: green, yellow and red colors represent 560 ppmv, 840 ppmv, and 1120 ppmv respectively. Grey color bars are the mean values of all the models. Different fill pattern

represent different geographic models, the blank and diagonal fill bars represent Robertsons and Getech Group Plc. Simulations respectively.

**Fig. 5** Difference between simulations and the fossil data for the Chattian period. The Y axes refers to the differences between modelling results and the fossil climate data (mean value of model data minus fossil data) for MAT, CMT, WMT, MAP, DryMP and WetMP respectively. The X axes show different simulation names. Different bar colors indicate different CO<sub>2</sub> level: blue, green, yellow and red colors represent 280 ppmv, 560 ppmv, 840 ppmv and 1120 ppmv respectively. Grey color bars represent mean values of all the models except ‘tedjm’ and ‘tecqa’. Different fill pattern bars represent different geographic models, the blank and diagonal fill bars represent Robertsons and Getech Group Plc. Simulations respectively.

**Fig. 6** The Rupelian (31 Ma) fossil data versus the ‘tecqn1’ HadCM3L simulation for MAT (A), CMT (B), WMT (C), MAP (D), DryMP (E) and WetMP (F). Grey color lines and dark thick lines on the map represent the present day and Oligocene land–sea boundaries respectively. Filled circles represent the fossil data while contoured map indicates the simulation data.

**Fig. 7** The Chattian (26 Ma) fossil data versus the ‘tedjp’ HadCM3L simulation. for MAT (A), CMT (B), WMT (C), MAP (D), DryMP (E) and WetMP (F). Grey color lines and dark thick lines on the map represent the present day and Oligocene land–sea boundaries respectively. Filled circles represent the fossil data while contoured map indicates the simulation data.

746 **Fig. 8** Vector winds and strength (m/s) at 850 hPa during the Rupelian ('tecqn1' simulation)

747 model in JJA (A) and DJF (B).



**Figure 1**  
[Click here to download high resolution image](#)

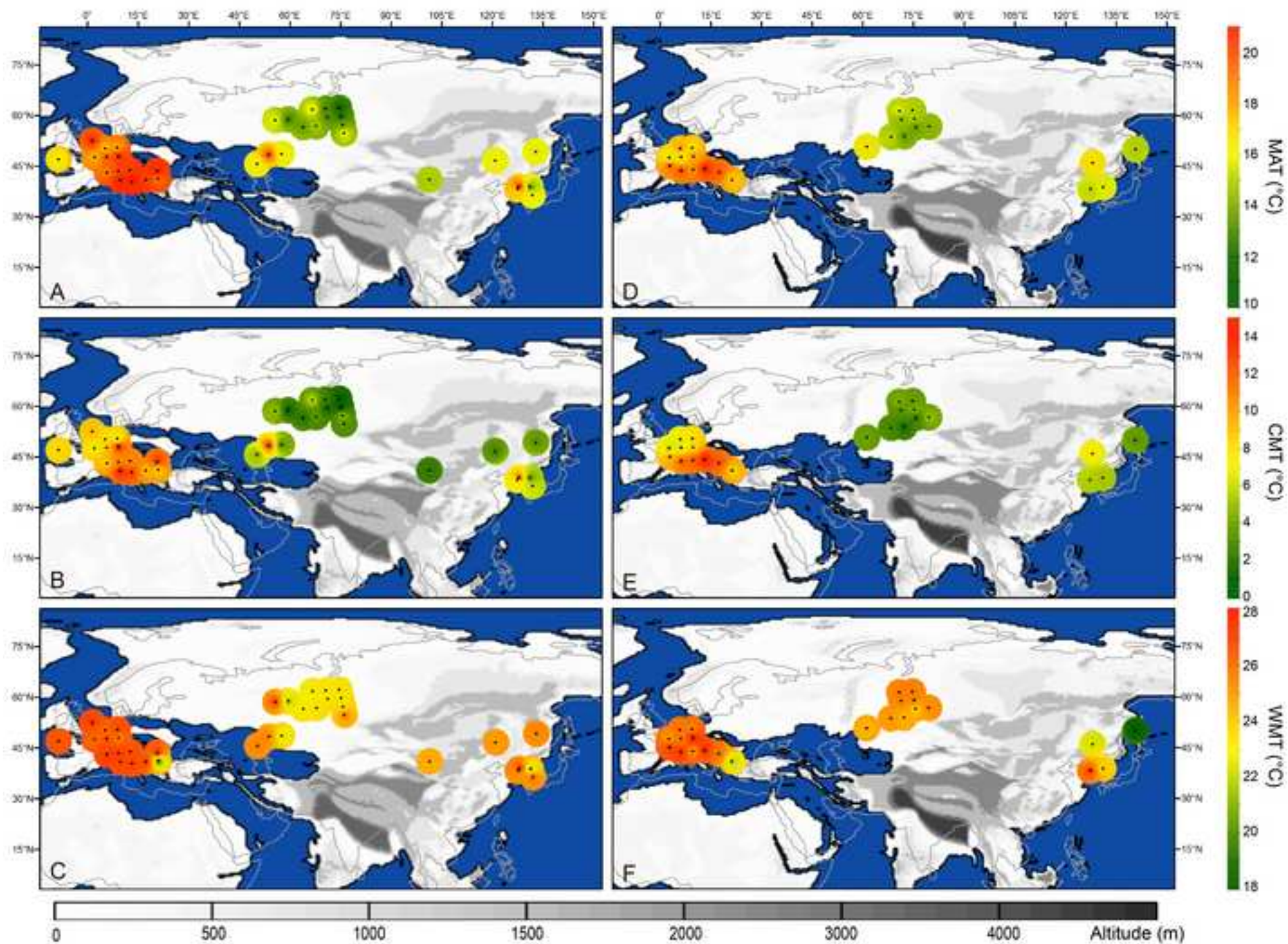




**Figure 2**  
[Click here to download high resolution image](#)

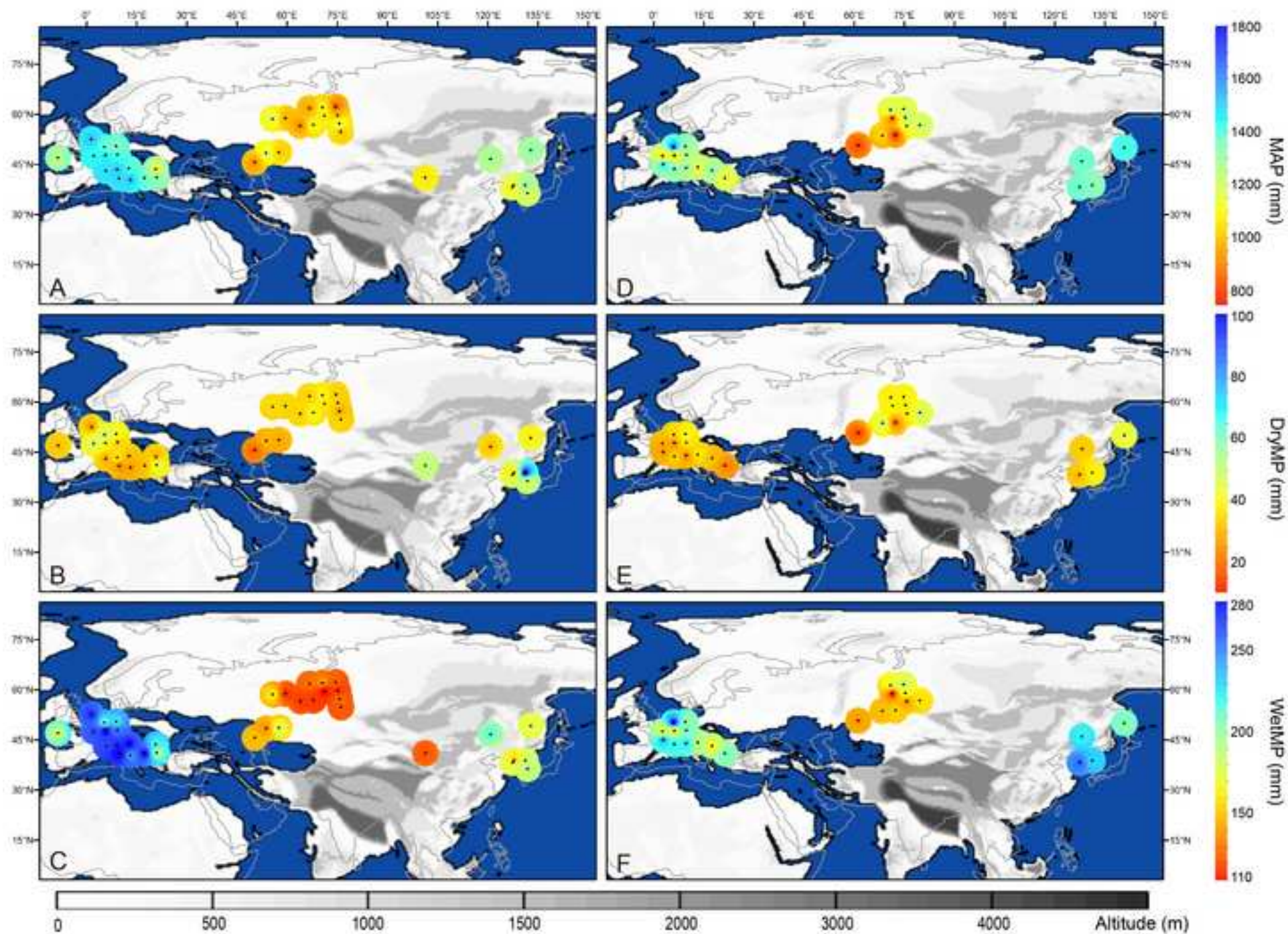




**Figure 3**  
[Click here to download high resolution image](#)

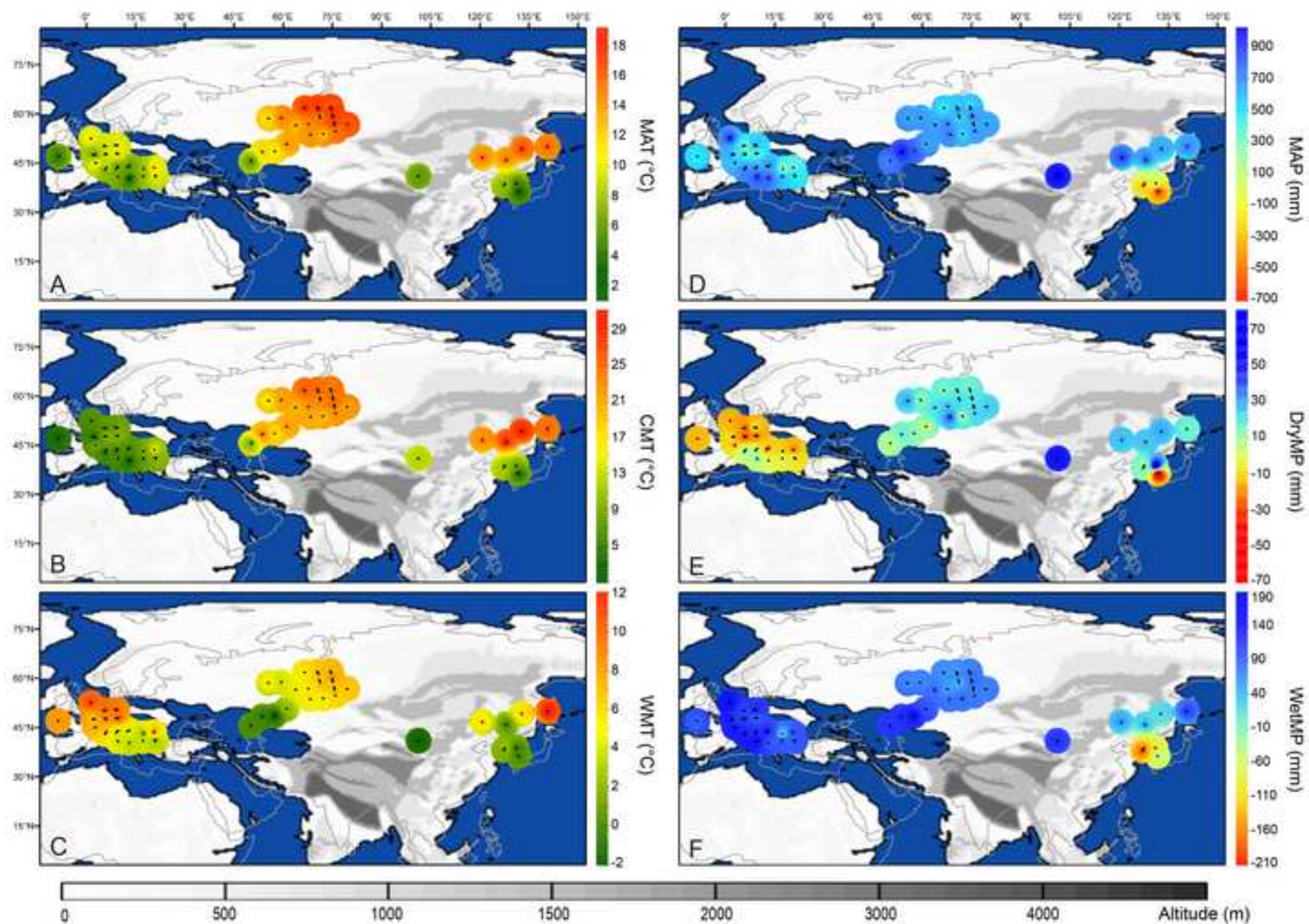


Figure 4

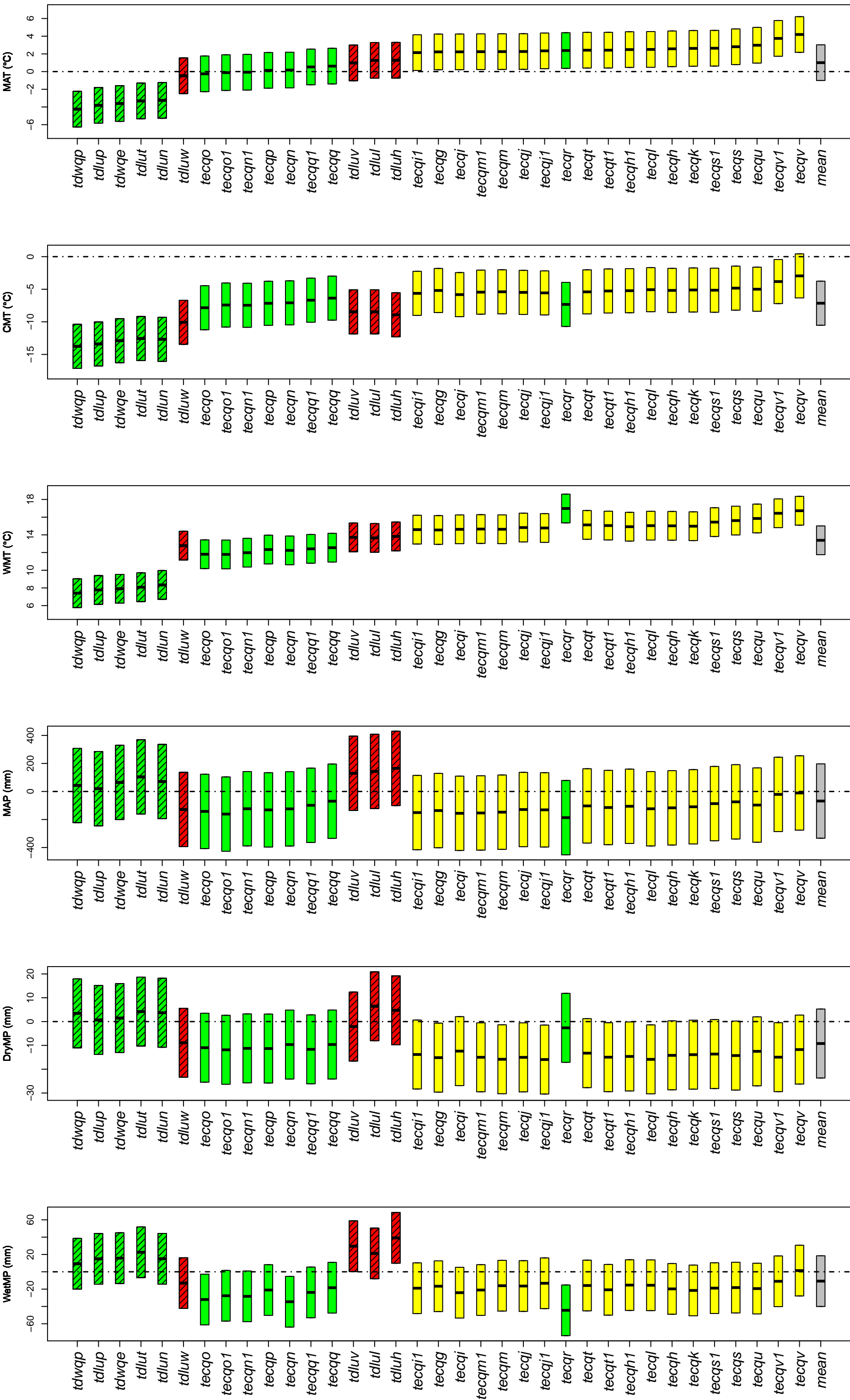
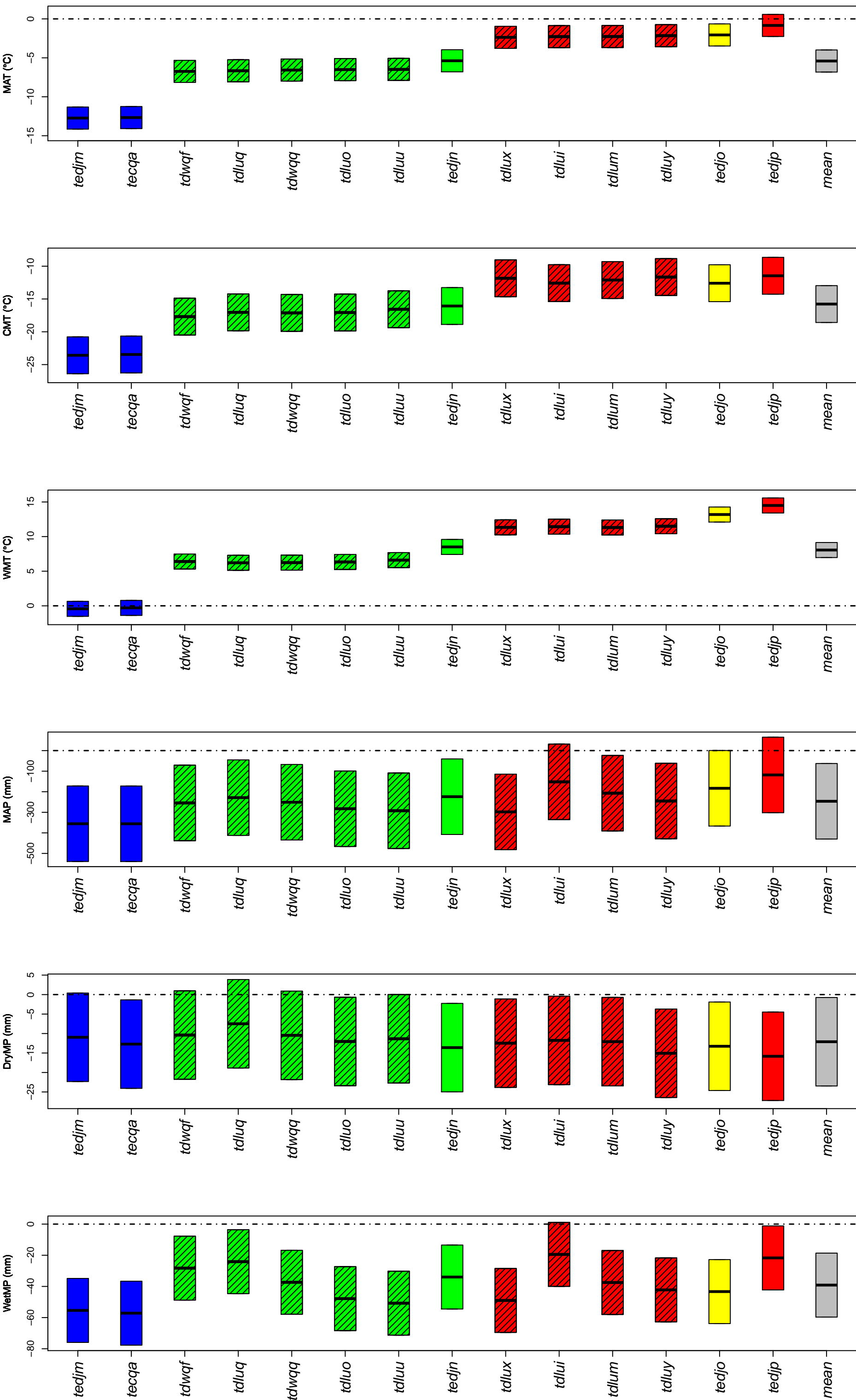
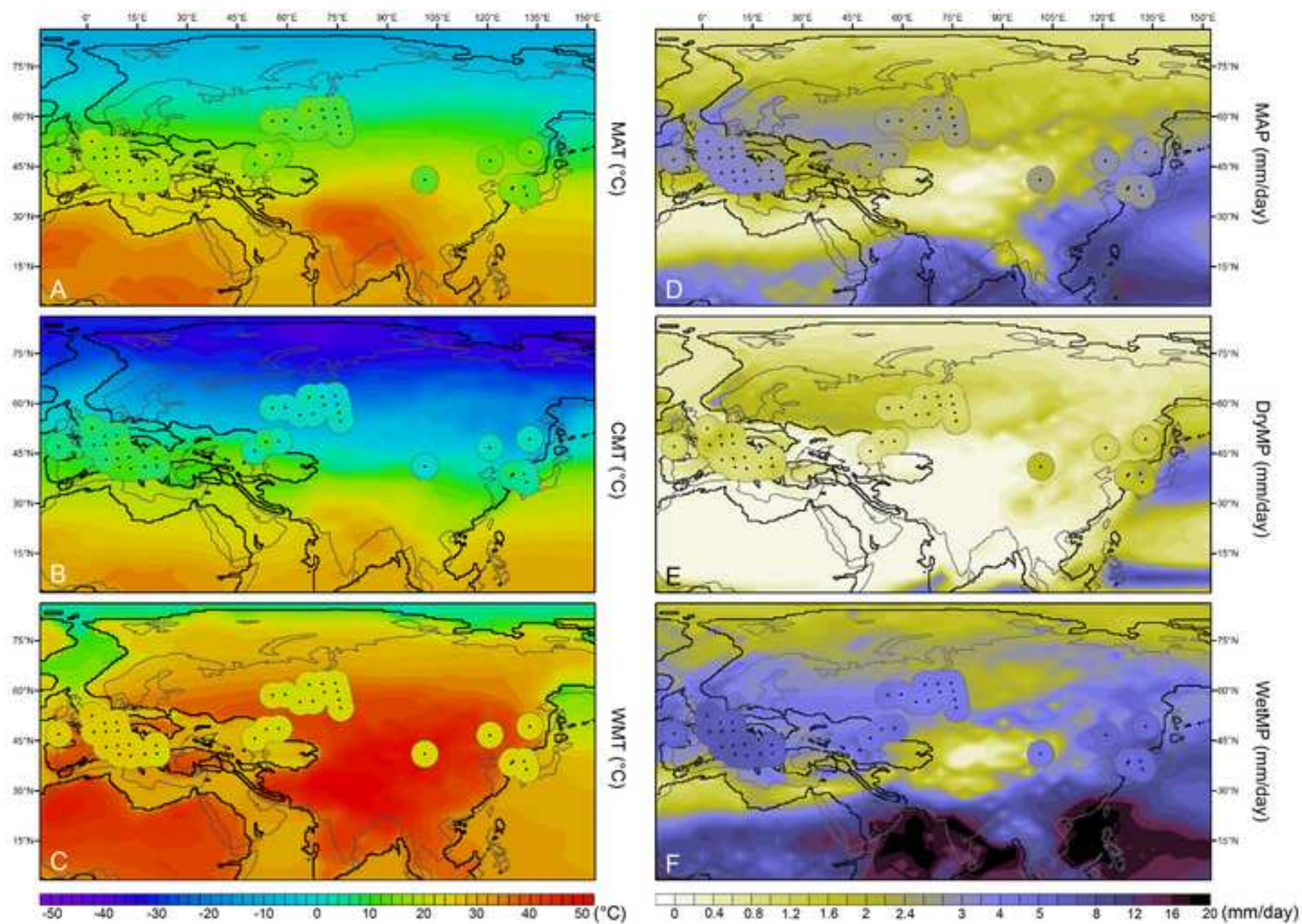


Figure 5





**Figure 6**  
[Click here to download high resolution image](#)





**Figure 7**  
[Click here to download high resolution image](#)

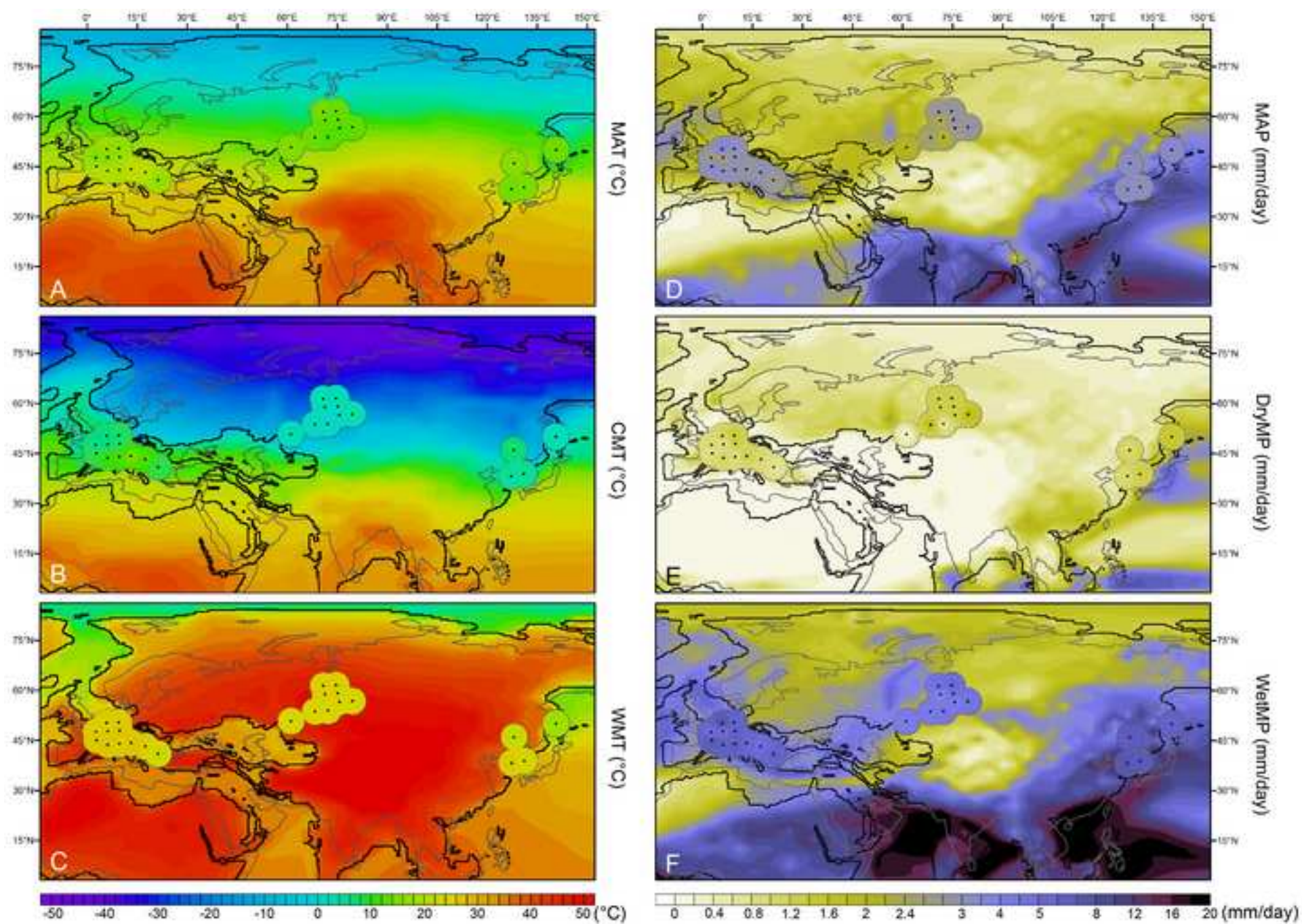




Figure 8  
[Click here to download high resolution image](#)

